

## NUMERICAL MODELING AND THEORETICAL CHARACTERIZATION OF EXPERIMENTAL PROCEDURES OF STEERER MAGNETS FOR PARTICLE ACCELERATORS

Daniel DAN<sup>1</sup>, Daniel IOAN<sup>2</sup>, Simona APOSTOL<sup>3</sup> and Ionel CHIRITĂ<sup>4</sup>

*The objective of this paper is to develop the theoretical characterization of experimental procedures (by magnetic measurements) of dipolar magnets for particle accelerators and numerical modeling of these procedures. The purpose of the modeling consist in numerical determination of the parameters that are to be measured.*

**Keywords:** magnets for particle accelerators, numerical modeling, magnetic field, theoretical characterization

### 1. Introduction

The objective of this paper is to develop the theoretical characterization of experimental procedures [1] (by magnetic measurements) of dipolar electromagnets for particle accelerators [2] and numerical modeling of these procedures. The Steerer type electromagnets are considered [3]. This type of electromagnet was designed in Jülich Research Centre in Germany and series production will be done by ICPE-CA. Magnets will be used at antiprotons and ions accelerator which will be built in Darmstadt, within FAIR the European project, where Romania is a partner.

A 3D view of the magnet is presented in Fig. 1.

#### 1.1. Specifications of the magnetic magnitudes of interest

- (1) Module dependence of the magnetic induction from the center of the electromagnet  $B_0$ , related to current intensity  $I = [0, 20, \dots, 280, 304]\text{A}$  (16 values, step  $\Delta I = 20\text{A}$ ) from the coil:

$$f_1(I) = B_0(I)/I. \quad (1)$$

- (2) Integral dependence of the transversal magnetic induction  $B_r$  along the electromagnet axis ( $Oz$  axis), related to the intensity of the current  $I$  from the

---

<sup>1</sup>PhD student, Faculty of Electrical Engineering, POLITEHNICA University of Bucharest, Romania, e-mail: [dan@lmn.ro](mailto:dan@lmn.ro)

<sup>2</sup>Professor, Faculty of Electrical Engineering, POLITEHNICA University of Bucharest, Romania, e-mail: [daniel@lmn.ro](mailto:daniel@lmn.ro)

<sup>3</sup> Research scientist, INCDIE ICPE-CA Bucharest, Romania, e-mail: [simona.apostol@icpe-ca.ro](mailto:simona.apostol@icpe-ca.ro)

<sup>4</sup>IDT2, INCDIE ICPE-CA Bucharest, Romania

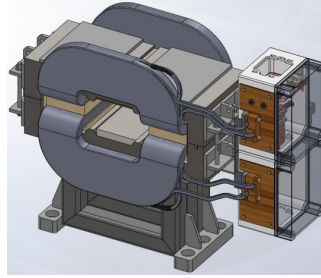


FIGURE 1. 3D SolidWorks modeling of the horizontal Steerer electromagnet designed by ICPE-CA

coil, as function of this intensity, for 16 values within the interval  $I = 0\text{A}$  and  $I = I_{\max} = 304\text{A}$ :

$$f_2(I) = \frac{1}{I} \int_{-\infty}^{+\infty} B_r(0, 0, z) dz \cong \frac{1}{I} \int_{-z_{\max}}^{+z_{\max}} B_r(0, 0, z) dz. \quad (2)$$

where  $B_r = \sqrt{B_x^2 + B_y^2}$  and  $z_{\max} = 5 \times 150 = 750\text{mm}$  [4] represents the distance measured on the longitudinal axis from the center of the magnet to the point where the magnetic field may be neglected.

(3) In order to characterize the transversal (horizontal) homogeneity the relative deviation of the horizontal magnetic induction is used, computed in various points of the  $Ox$  axis (from  $-x_{\max}$  to  $x_{\max} = 50\text{mm}$ ), relative to its value from the center of the device:

$$f_3(x) = \Delta B/B = (B_x(x, 0, 0) - B_0)/B_0, \quad (3)$$

where the magnetic induction is evaluated for  $I_{\max}$  and  $y = 0\text{mm}$ ,  $z = 0\text{mm}$ .

(4) Dependence of the effective magnetic length  $L_{ef}$  on the current intensity  $I$  [4].

$$f_4(I) = L_{ef}(I) = \frac{1}{B_0} \int_{-\infty}^{\infty} B_r(0, 0, z) dz \approx \frac{1}{B_0} \int_{-z_{\max}}^{z_{\max}} B_r(0, 0, z) dz, \quad (4)$$

function that is defined within the interval  $I = 0\text{A}$  to  $I_{\max} = 304\text{A}$ .

(5) The value of the electromagnet inductance which should have the value  $f_5 = L = 0.28\text{mH}$ .

## 2. 2D magnetic modeling

COMSOL specialized program based on the finite element method (FEM) was used for modeling.

A  $Oxyz$  Cartesian coordinate system was attached to the device with the origin  $O(0, 0, 0)$  in the center of the device,  $Ox$  its the horizontal axis,  $Oy$  its vertical axis and  $Oz$  its longitudinal axis. The  $Oz$  axis is oriented in the direction of the particle stream.

## 2.1. Geometric model and Modeling hypotheses

A 2D plane-parallel problem is considered, with a cross section ( $xOy$  plane) of the electromagnet depicted in Fig. 1. In this model, we considered  $z = 0$ . Domain consists of homogeneous subdomains: soft iron (Fe), Copper (Cu) and insulating materials (Air, Water). The structure has two axes of symmetry: horizontal axis  $Ox$  (the field lines are perpendicular on it) and the vertical axis  $Oy$  (where the field lines are tangential). Only a quarter of the cross section of the magnet was analyzed (quarter plan  $x < 0, y > 0$ ) (Fig. 2).

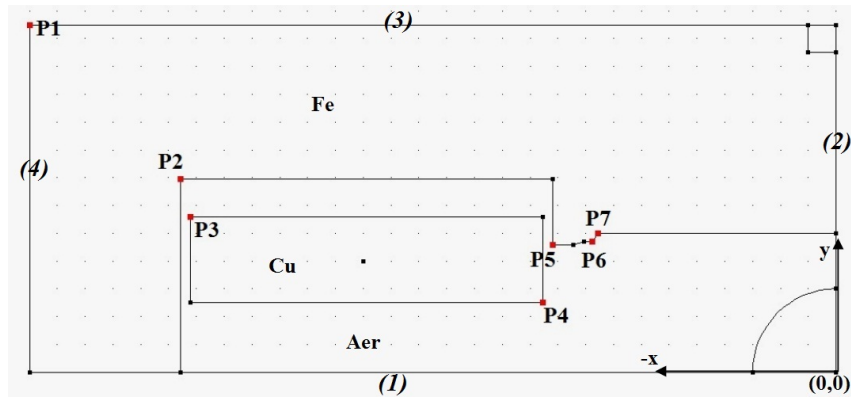


FIGURE 2. 1/4 of the cross section of the Steerer magnet

|     | $P_1$ | $P_2$  | $P_3$  | $P_4$  | $P_5$   | $P_6$    | $P_7$   |
|-----|-------|--------|--------|--------|---------|----------|---------|
| $x$ | 0.29  | 0.2356 | 0.2321 | 0.1055 | 0.102   | 0.08759  | 0.08561 |
| $y$ | 0.125 | 0.0695 | 0.056  | 0.025  | 0.04596 | 0.046879 | 0.045   |

TABLE 1. Value of geometric parameters ( $P_1 - P_7$  points coordinates in  $m$ )

The geometrical simplifications are: simplification of the ferromagnetic armature, assimilation of insulating components, elimination of all technological details and clamping.

The electromagnet is traversed by a Direct Current, this being the magnetic field source for the considered problem. Therefore a stationary magnetic field is assumed. The maximum current density is  $J_{max} = (44 \cdot 304) / (0.003925) = 3.4e6 A/m^2$ , where  $I_{max} = 304 A$ , number of windings is 44, area of the cross section of coil  $A_{fir} = 0.003925 m^2$ .

The yoke of the magnet consists of two  $E$  shaped glued stacks, made from low carbon steel laminations with thickness  $g = 1 \text{ mm}$ . Data for the imposed magnetization curve for this material (soft iron) can be seen in Table. 2.

TABLE 2. Data for first magnetization curve ( $\mathbf{BH}$  ).

|                 |      |      |       |       |        |
|-----------------|------|------|-------|-------|--------|
| $B[\text{T}]$   | 0.12 | 1.45 | 1.70  | 1.80  | 2.0    |
| $H[\text{A/m}]$ | 50   | 700  | 4,000 | 8,000 | 25,000 |

## 2.2. The mathematic model

We consider the 2D parallel plane problem, where the magnetic field is described by the magnetic flux density  $\mathbf{B}$  and that satisfy the stationary magnetic field equations [5], [6]:

$$\operatorname{div} \mathbf{B} = 0; \operatorname{rot} \mathbf{H} = \mathbf{J}; \mathbf{B} = \mathbf{f}(\mathbf{H}), \quad (5)$$

where we have: Magnetic flux density:  $\mathbf{B}(x, y) = \mathbf{i}B_x(x, y) + \mathbf{j}B_y(x, y)$ , with  $\mathbf{B} : \Omega \rightarrow \mathbb{R}^2$ ; Magnetic field strength:  $\mathbf{H}(x, y) = \mathbf{i}H_x(x, y) + \mathbf{j}H_y(x, y)$ , with  $\mathbf{H} : \Omega \rightarrow \mathbb{R}^2$ ; Current density:  $\mathbf{J}(x, y) = \mathbf{k}J(x, y)$ , with  $J : \Omega \rightarrow \mathbb{R}$ ; Magnetization characteristic  $\mathbf{f}(\mathbf{H}) = \mu_0\mu_r \mathbf{H}$  with  $\mathbf{f} : \mathbb{R}^2 \rightarrow \mathbb{R}^2$ . Each subdomain will be assumed to be homogeneous, having the same source field in all of its points.

Since the magnetic induction is solenoidal, it admits a potential magnetic vector, which we will consider solenoidal, according to Coulomb calibration:

$$\mathbf{B} = \nabla \times \mathbf{A}; \nabla \mathbf{A} = 0. \quad (6)$$

The potential vector satisfies the nonlinear second order differential equation:

$$\nabla \times \mathbf{g}(\nabla \times \mathbf{A}) = \mathbf{J}; \quad (7)$$

where  $\mathbf{g} : \mathbb{R}^2 \rightarrow \mathbb{R}^2$  is the inverse of  $\mathbf{f}$  function, presumed as bijective, so that  $\mathbf{f} \circ \mathbf{g}$  represents the identity function.

For the 2D case we have  $\mathbf{A}(x, y) = \mathbf{k}A(x, y)$  with  $A : \Omega \rightarrow \mathbb{R}$  and that satisfies the generalized Poisson's equation div-grad type:

$$\nabla \cdot \mathbf{g}(\nabla \cdot A) = J \Rightarrow \nabla \cdot (\nu \nabla \cdot A) = J_t. \quad (8)$$

This equation has the following zero boundary conditions:

$$\mathbf{B}_n = \mathbf{n} \cdot \mathbf{B} \text{ on } S_B \subset \partial\Omega; \mathbf{H}_t = 0 \Leftrightarrow -dA/dn = B_{rt} \text{ on } S_H = \Omega - S_B. \quad (9)$$

The boundary conditions are according to Fig. 2: for 2 – 4:  $A = 0$  (Dirichlet); for 1:  $dA/dn = 0$  (Neumann).

## 2.3. Solving. Post processing. Results

Steerer electromagnet has been modeled with COMSOL finite elements package 3.5 version [7]. Magnetic induction spectrum (left side) together with magnetic induction modulus variation along  $x$  negative semiaxis at  $z = y = 0\text{mm}$  for a maximum current  $I_{\max} = 304\text{A}$  (right side) can be seen in Fig. 3.

The computation implied solving a nonlinear problem for  $T = 49088$  triangles discretization and third order Lagrange polynomial with 221509 degrees of freedom [4]. The value of the central magnetic induction at a maximum current value is  $B_0 = 0,329\text{T}$ .

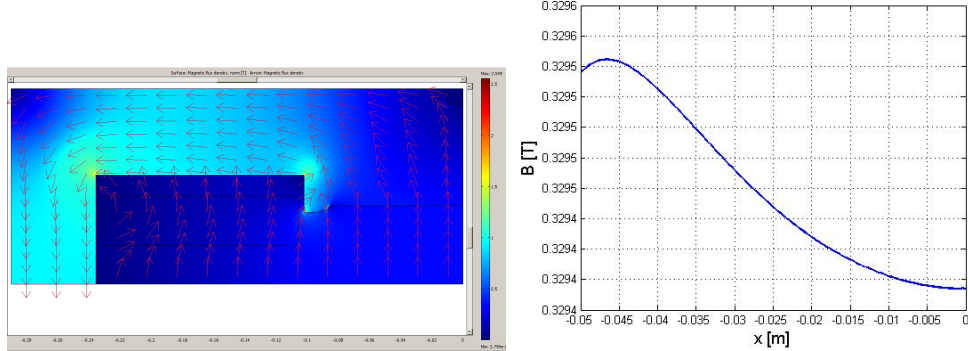


FIGURE 3. Magnetic induction spectrum (left) and magnetic induction modulus variation along  $x$  negative semiaxis (right)

For the local excitation curve (related central induction) the magnetic induction components  $\mathbf{B} = (B_x, B_y, B_z) = (B_{x,0}, B_{y,0}, B_{z,0})$  have been determined together with the modulus:  $B_0 = |\mathbf{B}| = \sqrt{B_x^2 + B_y^2 + B_z^2} = \sqrt{B_{x,0}^2 + B_{y,0}^2 + B_{z,0}^2}$ , in the point with coordinates  $P(x, y, z) = P_0(0, 0, 0)$  for different values of the electric current  $I$ . The numerical results are presented in Figure 4 (left side).

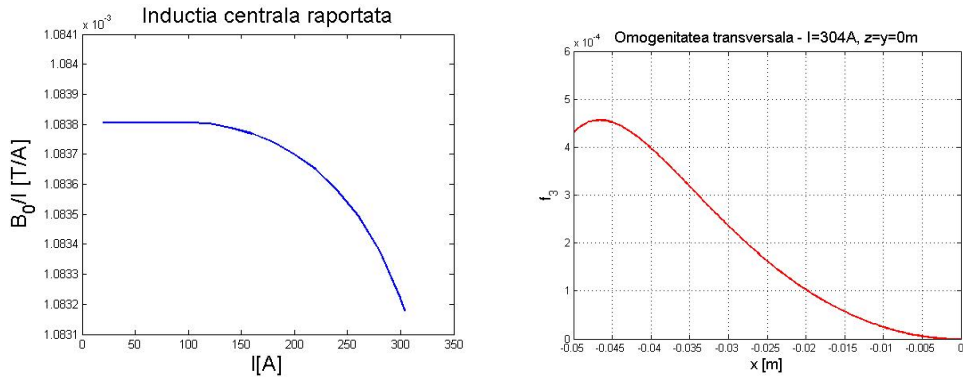


FIGURE 4. Related central induction (left) and Relative deviation (right)

For the local homogeneity the transversal homogeneity has been determined according to formula (3) and the results are presented in Fig. 4.

### 3. 3D models of the Steerer electromagnet

The tridimensional geometric model will consider the entire geometry (Fig. 5 - stânga). Due to symmetry a field analysis can be made only considering 1/8 from the electromagnet domain (Figure 5 - right).

The geometry of the device together with the computing domain were designed in Solidworks and imported in COMSOL software (Fig. 6).

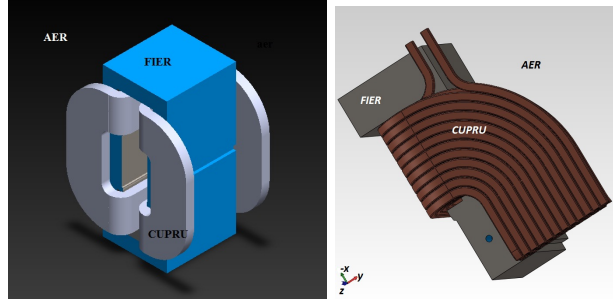


FIGURE 5. 3D view of the Steeree electromagnet (left) and the computing domain - Solidworks geometry (right)

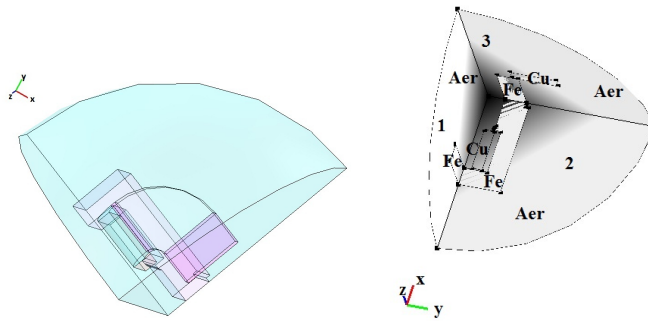


FIGURE 6. 3D geometry in COMSOL (left) and boundaries of the 3D computing domain (right)

### 3.1. Physical modeling and mathematical model

The modeling hypothesis form the 2D modeling also apply for the 3D case.

The stationary magnetic field from the  $\Omega \subset \mathbb{R}^3$  domain will be determined, considering one eighth of a sphere with  $R$  radius, presented in Fig. 6 and containing the disjunctive subdomains  $\Omega_{Fe}$ ,  $\Omega_{Cu}$  si  $\Omega_{Ae}$ . In the 3D problems, this is described by the magnetic induction which is a tridimensional vectorial field:  $\mathbf{B}(x, y, z) = \mathbf{i}B_x(x, y, z) + \mathbf{j}B_y(x, y, z) + \mathbf{k}B_z(x, y, z)$ , defined on  $\Omega$  with  $\mathbf{B} : \Omega \rightarrow \mathbb{R}^3$  and which satisfies, as in the 2D case, the fundamental ecuations of the stationary magnetic regime (5), where, this time, the intensity of the magnetic field is  $\mathbf{H} : \Omega \rightarrow \mathbb{R}^3$ , and the current density is  $\mathbf{J}(x, y, z) = \mathbf{i}J_x(x, y, z) + \mathbf{j}J_y(x, y, z) + \mathbf{k}J_z(x, y, z)$ , cu  $\mathbf{J} : \Omega \rightarrow \mathbb{R}^3$ , with the magnetizing characteristic  $\mathbf{f} : \mathbb{R}^3 \rightarrow \mathbb{R}^3$ .

A magnetic vector potential  $\mathbf{A} : \Omega \rightarrow \mathbb{R}^3$  is considered as in the 2D case. The magnetic vector potential satisfies the nonlinear second order differential equation (7), where  $\mathbf{g} : \mathbb{R}^3 \rightarrow \mathbb{R}^3$  is the inverse of the  $\mathbf{f}$  function. In the particular case of the environments with linear magnetic characteristic, the magnetic vector potential satisfies in the 3D case the linear Poisson equation:  $\text{rot}(\nu \text{rot} \mathbf{A}) = \mathbf{J}$ ; with the boundary conditions for the normal component of the magnetic induction  $B_n$ :  $\mathbf{n} \cdot \mathbf{B} =$

0 pe  $S_B \Rightarrow \mathbf{n} \times \mathbf{A} = 0$  pe  $S_B$ , and for the tangential component of the magnetic field intensity  $\mathbf{H}_t$ :  $\mathbf{n} \times \mathbf{H} = \mathbf{J}_s \Rightarrow \mathbf{n} \times (\nu \operatorname{rot} \mathbf{A}) = \mathbf{J}_s$  pe  $S_H = \partial\Omega \setminus S_B$ .

The computing domain is presented in Figure 6. Because face 1 (Fig. 6) with  $y = 0$  boundary is perpendicular to the magnetic field lines, this belongs to  $S_H$  (Boundary conditions are Neumann type), while faces 2 and 3, with  $z = 0$  and respectively  $z = 0$  as boundaries, these being field surfaces, they belong to  $S_B$  (Boundary conditions are Dirichlet type). The symmetry plans have perfect magnetic conductor (PMC) boundary conditions on face 1 and, respectively, perfect magnetic insulator (PMI) boundary condition on face 2 and 3. The rest of the boundary must be placed sufficiently far to have a neglectable magnetic field.

### 3.2. Problem solving. Solution validation

Numerical modeling has as purpose discretizing the field problem previously formulated in order to study the magnetic field variation along the  $Oz$  axis for validating the 2D solution.

The results are presented in Figure 7, which describes the field variation along the  $Oz$  for two different discretizations with 17507 elements (115084 freedom degrees) and 74376 elements (482544 freedom degrees).

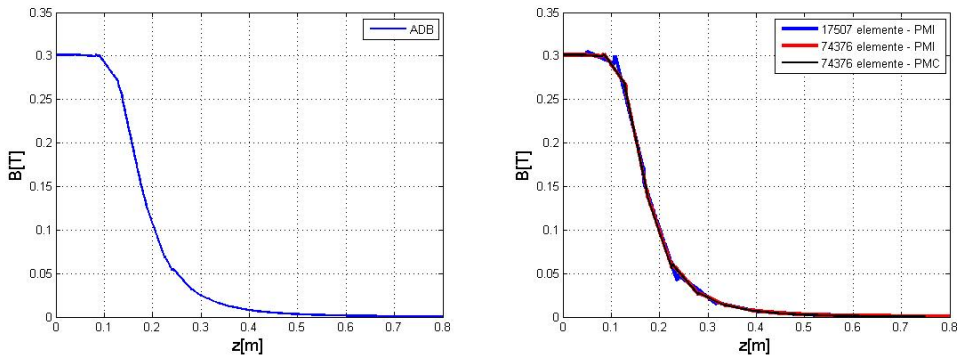


FIGURE 7. Magnetic induction variation along the  $Oz$  axis for  $I_{\max} = 304, 1\text{A}$ , with the dual boundary condition (ADB) (left) and Magnetic induction variation along the  $Oz$  axis for  $I_{\max} = 304, 1\text{A}$ , for both cases (right)

The magnetic field lines can be seen in Figures 8 (left).

Magnetic field inductance variation along the  $Ox$  can be seen in Figure 8 (right), where this variation is compared to the one from the 2D modeling.

In order to increase the trust degree for these numeric results, the effect of the fictitious boundary will be studied. If the condition on this boundary is changed from PMI in PMC, the magnetic field will be as in Figure 7 (right), and the magnetic induction from the center of the electromagnet increases with 0,0713%, which validates the position of the fictitious boundary as being far enough (radius  $R = 0,8\text{m}$ ).

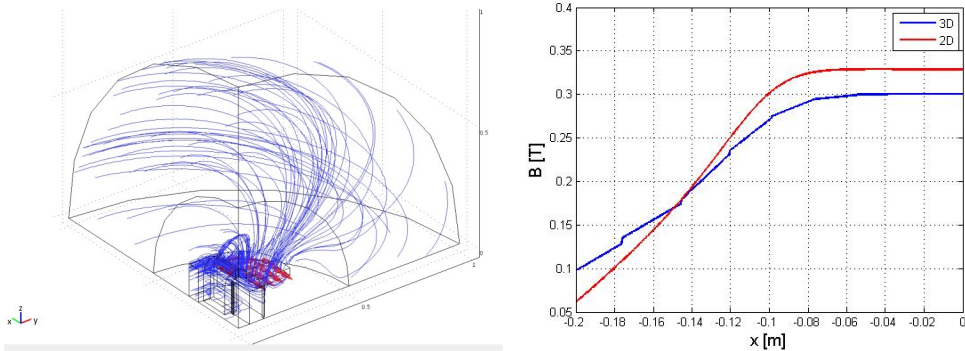


FIGURE 8. Magnetic field lines (left) and Induction variation along  $Ox$  axis (right)

Figure 7 (left) presents the field variation along  $Oz$ , computed as the mean of the two solutions PMI and PMC.

In graph 9 the magnetic induction can be seen along the  $Oz$  axis for 17 values of the current  $I$ .

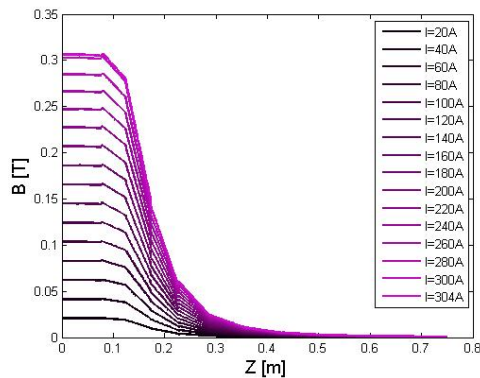


FIGURE 9. Variation of the magnetic induction along the  $z$  axis with  $I$  as parameter

**3.2.1. Postprocessing. Results.** The purpose of the 3D Steerer electromagnet modeling is the study of the magnetic field behaviour along the  $Oz$  axis of this electromagnet, on distance  $z \in [-750, 750]$ mm and  $x = y = 0$ mm .

*The average transversal induction* has been determined as following:

- The transversal component of the magnetic induction was determined  $B_r = \sqrt{B_x^2 + B_y^2}$  in  $N = 150$  points  $P_j(0, 0, z_j)$  placed equidistantly along  $Oz$  axis of the electromagnet, on the interval  $z \in [-750, 750]$ mm, with a step  $h = 10$ mm. More exactly in  $P_k$  points for which:

$$z = [\pm 750, \pm 740, \dots, \pm 30, \pm 20, \pm 10, 0], \quad (10)$$

- The average value of the induction  $B_r$  for 151 points on the  $Oz$  axis with the result  $\tilde{B}_r^m$ , which has been reported to the value of the coil current in order to obtain the transversal excitation factor (IEC);
- Repeated the above for 16 of the electric current in the interval  $I = [0, 304]\text{A}$ .

Using "Trapezoidal numerical integration" [8] from Matlab for each current  $I_k$ , the integral  $\tilde{B}_{r,k}$ ,  $k = 1, \dots, 17$  of the transversal magnetic induction  $B_r$  was computed and reported to intensity  $I_k$  according to the formula (2).

The dependence of the magnetic induction integral on the current is presented in Figure 10 (left), and the graph of the  $f_2(I)$  function is presented in Figure 10 (right).

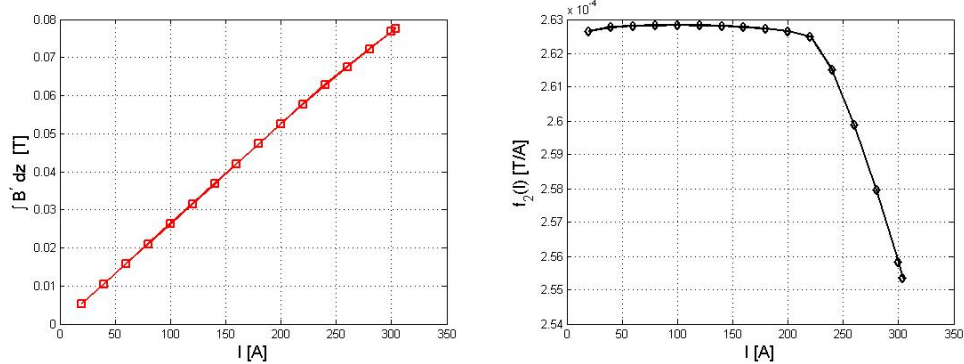


FIGURE 10. Induction integral along  $Oz$  axis (left) and average transversal induction,  $y = 0\text{mm}$  (right)

One can observe a decrease of the excitation factor, for values higher than 200A which is justified by the saturation of the magnetic core (a nonlinear model being used).

#### 4. Magnetic circuite approximative model

For the approximative determination of the magnetic field distribution generated by systems of coils placed on magnetic cores, the most frequent method is that of magnetic circuits [9], Fig. 11.

Since  $\mathbf{B} = \mu_0 \mu_r \mathbf{H}$ , in the linear case, the reluctance can be computed by using the formula:  $R_{lin} = L / (A \mu_0 \mu_r)$  [ $\text{H}^{-1}$ ]. Where,  $L$  [m] is the length of the section is,  $A$  [ $\text{m}^2$ ] is the area of the selection section and  $\mu_0 = 4 \cdot \pi \cdot 10^{-7}\text{H/m}$ , with  $\mu_{Air} = \mu_{Cu} = 1$  in air and in copper. The iron magnetic permeability shall be considered as  $\mu_{Fe} = 344$ .

Magnetic reluctance of this magnetic circuit has the following values:

$$R_{m1} = R_{Fe1} = |(y_2 + y_1)/2| / (\mu_0 \cdot \mu_{Fe} \cdot |x_1 - x_2| \cdot L_{jm}) = 0,0153 \cdot 10^6 \text{H}^{-1};$$

Where  $L = [(y_2 - y_0) + (y_1 - y_0)]/2 = (y_2 + y_1)/2$ , since  $y_0 = 0\text{m}$ .

$$R_{m2} = R_{Fe2} = |(x_2 + x_1)/2| / (\mu_0 \mu_{Fe} \cdot |y_2 + y_7 - 2y_1| \cdot L_{jm}) = 0,0166 \cdot 10^6 \text{H}^{-1}.$$

Where:  $L = [(x_2 - x_0) + (x_1 - x_0)]/2 = (x_2 + x_1)/2$ . Here  $x_0 = 0\text{m}$ . The length

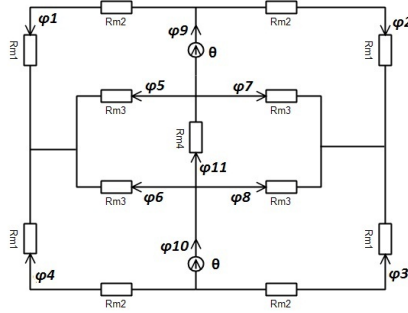


FIGURE 11. Magnetic circuit

of the section is the sum  $(y_2 - y_1) + (y_7 - y_1) = y_2 + y_7 - 2y_1$ .  $R_{m3} = R_{Cu} = y_2/(\mu_0 \cdot \mu_{Cu} |x_2 - x_5| L_{jm}) = 1.5332 \cdot 10^6 \text{ H}^{-1}$ ,  $R_{m4} = R_{Air} = y_7/(\mu_0 \cdot \mu_{Cu} \cdot x_5 \cdot L_{jm}) = 1.4 \cdot 10^6 \text{ H}^{-1}$ ,

The coils have the following values  $\Theta = nI_{max} = 44 \cdot 304 = 13376 \text{ Asp}$  for  $I_{max}$ .

Form the symmetry there will be:  $\varphi_1 = \varphi_2 = -\varphi_3 = -\varphi_4 = \varphi_9/2 = 18,8 \text{ mWb}$ ,  $\varphi_9 = \varphi_{10} = 37,6 \text{ mWb}$ ,  $\varphi_6 = \varphi_8 = -\varphi_5 = -\varphi_7$ .

One can see that:

$\varphi_9 = 2\theta/(R_{m12} + R_{m34}) = 37,6 \text{ mWb}$ ,  $\varphi_{11}/2 = 0.5\varphi_9 R_{m3}/(R_{m4} + R_{m4}) = 20 \text{ mW.b}$ , cu  $R_{m12} = R_{m1} + R_{m2} = 31,9 \cdot 10^3 \text{ H}^{-1}$ ;  $R_{m34} = R_{m3} R_{m4}/(R_{m3} + R_{m4}) = 0,7 \cdot 10^6 \text{ H}^{-1}$

The magnetic induction from the center of the electromagnet and the coil inductance have the values:  $B_0 = 0,5\varphi_{11}/A = 0,36 \text{ T}$ ,  $L = N \cdot \varphi_9/I = 5,44 \text{ mH}$ , and if one considers both sections of the coil, then the series inductivity is double.

## 5. Effective magnetic length

According to [10], the approximative value of the magnetic length of the Steerer dipole can be computed with:

$$L'_{mg} \approx l_{Fe} + 2 \cdot h \cdot k = 270 + 2 \cdot 100 \cdot (0,3 \div 0,6) = (0,33 \div 0,39) \text{ m}, \quad (11)$$

where  $l_{Fe} = 270 \text{ mm}$  is the iron thickness (magnetic yoke),  $h = 100 \text{ mm}$  is the distance between the two poles and  $k = 0,3 \div 0,6$  is an empiric constant.

Using the average:

$$l_{mg} = \int_{-\infty}^{\infty} \frac{B(z)dz}{B_0} \cong \int_{-z_{max}}^{z_{max}} \frac{B(z)dz}{B_0} = 0,38 \text{ m}, \quad (12)$$

the value is within the interval  $(0,33 \div 0,39)$ .

In order to estimate the effect of the integral truncation (12), the asymptotic expression of the magnetic field is considered, field generated by a coil, at long distance on coil's axis.

Any finite dimensions coil is known to produce in vacuum, at a relatively long distance, a magnetic field whose intensity has a asymptotic variation related to distance  $R$  form the center of the winding to the point where the field is estimated which is similar to the one of a punctiform magnetized body [11]:

$$\mathbf{H} = -\nabla V_m \text{ cu } V_m = \mathbf{m} \cdot \mathbf{R} / (4\pi R^3) = (m \cdot \cos \theta) / (4 \cdot \pi \cdot R^2), \quad (13)$$

where  $V_m$  is the magnetic scalar potential and  $\mathbf{m}$  is the magnetic moment of the coil. Thus, there will be only the radial component of the magnetic field intensity:

$$H_R = -\partial V / \partial R = 2 \cdot m \cdot \cos \theta (4\pi R^3)^{-1} = m / (2 \cdot \pi R^3), \quad (14)$$

the angular component is null at  $\theta = 0^0$ . Magnetic induction  $\mathbf{B} = \mu_0 \mathbf{H}$  has the following expression:  $B = m \mu_0 \cdot (2 \cdot \pi \cdot z^3)^{-1}$ . If the coil is composed of one plan winding with area  $A$ , traversed by current  $I$ , then its moment is  $m = I \cdot A$ . The modulus value of this moment will be estimated using the magnetic induction form  $z = z_{\max}$  position, on the  $Oz$  axis:  $m = B(z_{\max}) 2\pi z_{\max}^3 \mu_0^{-1} = 3398 \text{ Am}^2$ . Integrating the asymptotic expression of the magnetic induction on the  $Oz$  axis, the following is obtained:

$$\tilde{B}'_r = \int_{z_{\max}=R}^{\infty} B dz = \int_R^{\infty} \frac{\mu_0 m}{2\pi R^3} dR = \frac{\mu_0 m}{4\pi z_{\max}^2} = 0.531 \text{ mNA}^{-1}. \quad (15)$$

Adding integrals contributions from  $z_{\max}$  to infinity, the following is obtained:

$$\tilde{B}''_r = \tilde{B}_r + 2 \cdot \tilde{B}'_r = 78.6 \text{ mNA}^{-1}.$$

The contribution of the imaginary component of the integral ( $z > z_{\max}$ ) has relative balance:  $x = 100 \tilde{B}'_r / \tilde{B}''_r \% \approx 0,676\%$ , which means that effective magnetic length computed by an integral on the limited interval  $(-z_{\max}, z_{\max})$  must be increased by  $2 \cdot x = 1.352\%$ . In the end, the value of the effective magnetic length is:  $l_{mg} = 0,3851376 \text{ m}$ .

## 6. Final results and conclusions

The 3D modeling has been validated by using two discretization networks. In the first case, with fewer freedom degrees, the magnetic induction in the center of the electromagnet is  $B_0 = B(0, 0, 0) = 0,301 \text{ T}$  and in the second case, with more freedom degrees, the value of the magnetic field is smaller with a factor of  $4,358 \cdot 10^{-5} \text{ T}$ . The relative deviation of 0,0145% between these two values validates the obtained numerical result.

Comparing the results from the 3D and 2D numeric modeling in terms of deviation a value of 8,5104% is obtained in the center of the electromagnet, but this gets higher as the magnetic core is reached, having values up to 10%. The justification for this is the dispersion along  $Oz$  of the field lines.

The curve for the functions (1), (2) și (3) have been represented. These theoretical curves resulted from the Steerer electromagnet modeling will be used as model for the magnetic characterization of the series production of the Steerer electromagnets for the particle accelerator. One can see that for a central induction of approx. 0.3T generated by a 304 current, a much higher value of the iron core coil induction is obtained than the one imposed by project requirements. The justification of this result is that the imposed value for the inductivity by the project is for the winding unmounted on the iron core.

The computed effective magnetic length is  $l_{mg} = 0,38\text{m}$ , and this value is in the imposed interval  $(0,33 \div 0,39)$ . Also, the integral (12) truncation effect has been determined and one can conclude that the effective magnetic length computed by an integral over the limited interval  $(-z_{\max}, z_{\max})$  must be increased by a factor of  $2 \cdot x = 1.352\%$ .

In the end, the value of the effective magnetic length is:  $l_{mg} = 0,3851376\text{m}$ .

## REFERENCES

- [1] S. Turner, *CAS - CERN Accelerator School: Magnetic measurement and alignment*. <http://cds.cern.ch/record/226263?ln=en>: CERN, 1992.
- [2] D. Brandt, *CERN Accelerator School Magnets*. <http://cas.web.cern.ch/cas/Belgium-2009/Bruges-advert.html>: CERN, 2009.
- [3] D. Dan, I. Chirită, N. Tănase, and S. Mălureanu, "Analysis, characterization and optimization of a steerer magnet prototype," *IEEE*, pp. 362 – 367, 2015.
- [4] I. Rodriguez and J. Munoz, "Benchmark of comsol vs. roxie codes for the calculation of a particle accelerator quadrupole," *Proceedings of IPAC10, Kyoto, Japan*.
- [5] M. Preda and F. S. P. Cristea, *Bazele Electrotehnicii (Basics of electrotechnics)*, vol. II. București, România: Editura Didactică și Pedagogică, 1980.
- [6] A. Timotin, V. Hortoman, A. Ifrim, and M. Preda, *Lecții de Bazele Electrotehnicii (Basics of electrotechnics lessons)*. București, România: Editura Didactică și Pedagogică, 1970.
- [7] Comsol, *AC/DC Module - User's Guide*. <http://www.mht.bme.hu/~bilicz/oktatas/mezoszim/ACDCModuleUsersGuide.pdf>, 2011.
- [8] Matlab, *Trapezoidal numerical integration*. <http://www.mathworks.com/help/matlab/ref/trapz.html>: Matlab, 2014.
- [9] D. Ioan, *Curs de Bazele Electrotehnicii (Basics of electrotechnics course)*. 2013.
- [10] T. Zickler, *Basic design and engineering of normal-conducting, iron-dominated electromagnets*, vol. 1. Geneva, Switzerland, 2012.
- [11] S. J. Wilhelm Kappel, Mirela-Maria Codescu, *Magneți Permanenți (Permanent Magnets)*. Ed. Printech, 2006.